Ultrasonic Propagation of a Metallic Domain in $Pr_{0.5}Ca_{0.5}CoO_3$ Undergoing a Photoinduced Insulator-Metal Transition

Y. Okimoto,[1] X. Peng,[1] M. Tamura,[1] T. Morita,[1] K. Onda,[1,2] T. Ishikawa,[1] S. Koshihara,[1,2] N. Todoroki,[3] T. Kyomen,[3,*] and M. Itoh[3]

[1]*Department of Materials Science, Tokyo Institute of Technology, Meguro, Tokyo, 152-8551, Japan*
[2]*Nonequilibrium Dynamics Project, ERATO/JST, Tsukuba, Ibaraki, 305-0801, Japan*
[3]*Materials and Structures Laboratory, Tokyo Institute of Technology, 4259 Nagatsuta, Yokohama, 226-8503, Japan*

(Received 30 September 2008; published 9 July 2009)

Femtosecond optical response was investigated on a perovskite-type cobalt oxide, $Pr_{0.5}Ca_{0.5}CoO_3$ during an insulator-metal (*I-M*) transition accompanied with the change in spin configuration. After photoirradiation at 30 K, the reflectivity showed a sudden and large increase with subsequent variation depending on the observed photon energy. An exact calculation of Maxwell's equations for the $Pr_{0.5}Ca_{0.5}CoO_3$ after the photoirradiation enabled us to observe the ultrafast dynamics of *I-M* phase transition and the motion of the photonically created metallic domain at the velocity of ultrasonic wave.

DOI: 10.1103/PhysRevLett.103.027402 PACS numbers: 78.47.J−, 71.27.+a, 71.30.+h, 74.25.Gz

Phase control aimed at finding a hidden phase with an intriguing function in a material is an important research topic in condensed matter physics today. The recent advances in femtosecond laser technology have led to photoirradiation being recognized as a novel tool for realizing and/or probing a latent phase [1]. The phase transition induced by light illumination is named as photoinduced phase transition (PIPT), and many PIPT candidates have been demonstrated, especially for so-called strongly correlated materials [2–4]. The PIPT phenomenon is generally accompanied by an ultrafast and/or large change in the refractive index of the material, and so it has attracted intense interest, particularly in the light of its application to ultrafast optical switching devices.

Among candidates of PIPT materials, perovskite-type manganese oxide is a typical one. The PIPT phenomenon in this class of materials, i.e., the phase change between the charge ordered insulating state and the ferromagnetic metallic state, was first observed by Miyano *et al.* [5]. This pioneering discovery was followed by several successive reports of ultrafast phenomena closely related to the PIPT phenomenon [6–10].

Here, we report for the first time an ultrafast and large photoresponse of a perovskite-type cobalt oxide, $Pr_{0.5}Ca_{0.5}CoO_3$ (PCCO). Cobalt perovskite has been studied in terms of the unconventional thermally induced spin state transition of the Co^{3+} cation in a CoO_6 octahedron [11]. This variation of the spin configuration in a strong crystal field is quite similar to that in spin-crossover complexes containing a transition metal element which are also an intriguing target in the study of PIPT [12]. From this viewpoint, the cobalt perovskite we investigated can be classified as a new class of PIPT material, i.e., a ''strongly correlated spin-crossover'' system, combining two of the main phenomena in solid state physics, i.e., the metal-insulator transition and the spin-crossover phenomenon.

We grew a polycrystalline sample of PCCO as described in a previous report [13]. PCCO has an insulator-metal transition temperature (T_{IM}) of ~89 K as first demonstrated by Tsubouchi *et al.* Figures 1(a) and 1(b) plot the temperature dependence of resistivity (ρ) and magnetic susceptibility (χ) derived from results previously reported for this system [13]. With a decrease in temperature, the ρ-T curve shows a sudden jump from a low resistive metallic (*M*) state to an insulating (*I*) state at around T_{IM}. The χ-T curve also shows a sudden jump at T_{IM}. These jumps are due to the transition from a low spin (LS) state ($S = 0$, $t_{2g}{}^6$) to an intermediate spin (IS) state ($S = 1$, $e_g{}^1 t_{2g}{}^5$) at the Co^{3+} sites. (Co^{4+} sites are always in an LS state, $t_{2g}{}^5$.) This assignment of the spin state is supported by the results of other studies [14–16].

The linear reflectivity spectrum [$R(\omega)$] was measured using a Fourier transform-type interferometer (0.01–0.7 eV) and a grating monochromator (0.6–5 eV). The relative change of reflectivity ($\Delta R/R$) caused by femtosecond laser pulse irradiation was obtained using the conventional pump-probe method. A Ti:sapphire regenerative amplified laser (pulse width ~120 fs, repetition rate 1 kHz, photon energy 1.58 eV) was used as a light source. The amplified light was divided into two paths; one was used as a pump light for the excitation, and the other as a probe light after the frequency was converted from 0.5 to 2.1 eV with an optical parametric amplifier.

To illustrate the overall electronic structure of PCCO, in Fig. 1(c), we show $R(\omega)$ at 290 and 30 K. At 290 K, it gradually increases with a decrease in the photon energy, suggesting metallic behavior ($dR/d\omega < 0$). At 30 K, in contrast, it decreases, especially below ~2 eV. Figure 1(d) illustrates the optical conductivity [$\sigma(\omega)$] at 290 and 30 K calculated by Kramers-Kronig (K-K) analysis. With decreasing temperature, the spectral weight in the midin-

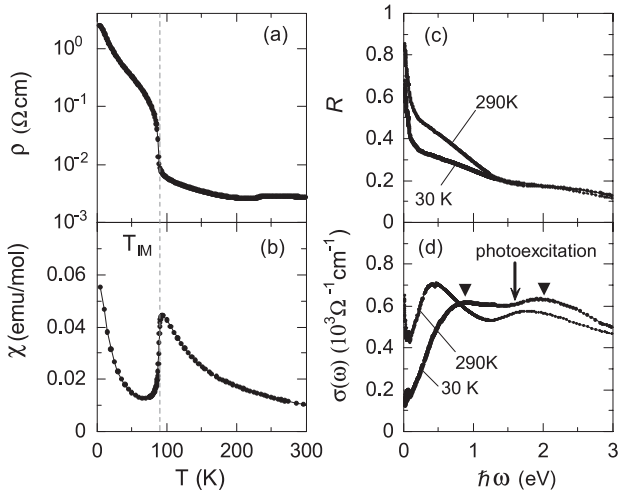

FIG. 1. (a),(b) Temperature dependence of resistivity (a) and magnetic susceptibility (b) in $Pr_{0.5}Ca_{0.5}CoO_3$. (c), (d) Reflectivity (c) and optical conductivity (d) spectra at 30 and 290 K. The arrow denotes the photon energy of the pump light (1.58 eV).

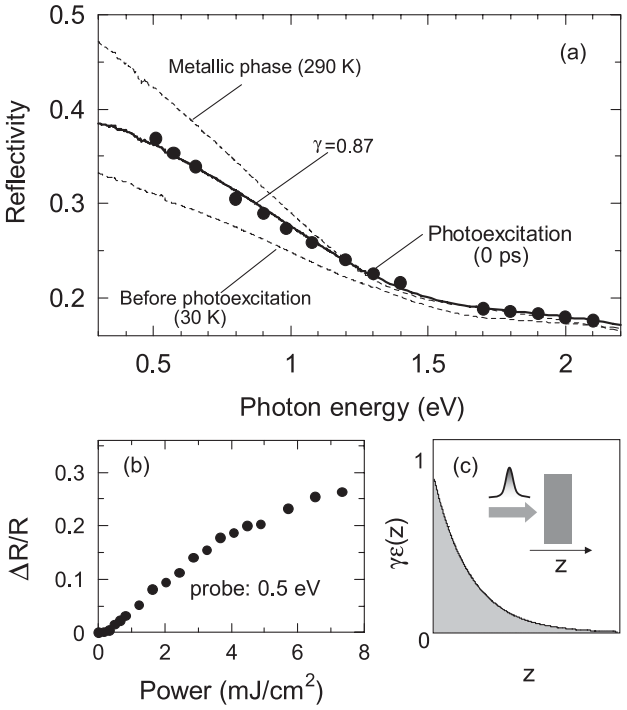

FIG. 2. (a) Reflectivity spectrum $[R(\omega)]$ just after photoexcitation (filled circles). For comparison, linear $R(\omega)$s at 30 and 290 K are plotted with solid lines. The bold line is the calculated $R(\omega)$ with $\gamma = 0.87$ (see text), which reproduced the experimental result. (b) Magnitude of the reflectivity change at 30 K of the excitation intensity of the pump light. (c) A schematic that accounts for the spatial variation of the dielectric function, $\varepsilon(z)$ with $\gamma = 0.87$ [see Eq. (1)].

frared region is suppressed, reflecting the gap opening in accordance with the *I*-*M* transition [17]. At 30 K, $\sigma(\omega)$ has two peaks, at ~1 and ~2 eV, as denoted by the upside-down triangles. These peaks can be assigned to the charge-transfer transitions from the O $2p$ band (hybridized with the Co t_{2g} states) to the empty Co t_{2g} band (~1 eV) and e_g band (~2 eV) [18]. The arrow shows the photon energy of the pump light (1.58 eV).

The spectrum of $\Delta R/R$ immediately after the photoirradiation (~0 ps) is plotted in Fig. 2(a) against the photon energy, 0.5–2.1 eV by closed circles. [The power density of the irradiated pump pulse was ~6 mJ/cm^2, which corresponds to ~0.15 photons per Co site. See also Fig. 2(b).] For comparison, we replotted the spectra of $R(\omega)$ at 30 K (*I*-phase) and at 290 K (*M*-phase) by broken lines. With the photoirradiation, $R(\omega)$ increased, and the spectral shape approached that of the metallic phase. $R(\omega)$ was comparable to or larger than the metallic spectrum above ~1.2 eV and was smaller below ~1.2 eV.

Figure 2(b) is excitation energy dependence of $\Delta R/R$ in the photon energy 0.5 eV at 30 K. The value of $\Delta R/R$ linearly increases with the pump power, and there was scarcely a threshold of excitation power, which is in contrast to the case of the vanadium dioxide [19].

K-K analysis of PCCO indicated that the penetration depth of the pump light (d) was so short (~60 nm) that the photonically created metallic state was not uniform along the depth of the sample. This indicates that the $R(\omega)$ of the probe light was determined not only by the dielectric function of the photoinduced metallic phase (ε^M) but also by that of the initial insulating state preserved even after the photoirradiation (ε^I).

To quantitatively clarify the spectral shape of the photoinduced $R(\omega)$ at ~0 ps, we assumed that the total dielectric function of the sample $\varepsilon(z)$, can be expressed by the following relation [20]:

$$\varepsilon(z) = \gamma \exp(-z/d)\varepsilon^M + [1 - \gamma \exp(-z/d)]\varepsilon^I. \quad (1)$$

Here, γ is the efficiency of the photoinduced phase transition ($0 < \gamma < 1$), and z is the distance from the sample surface. The first component is induced by the photoirradiation, as schematically depicted in the inset of Fig. 2(c). We assumed that ε^M corresponds to ε at 290 K, and ε^M and ε^I can be derived by K-K analysis of the linear $R(\omega)$ spectra. Once the $\varepsilon(z)$ is determined, we can calculate the Fresnel coefficient and hence $R(\omega)$ on the surface ($z = 0$) as a function of γ [21]. Then, we can fit the photoinduced spectrum in terms of the least squares analysis using Eq. (1), indicating that $\gamma = 0.87 \pm 0.14$. In Fig. 2(a) we show the calculated $R(\omega)$ with $\gamma = 0.87$ by a bold line, which well reproduces the observed photoinduced spectrum. This clearly indicates the creation of a photoinduced metallic state just after the photoirradiation (i.e., on the femtosecond time scale) as well as the z dependence of ε, as expressed in Eq. (1).

The photon energy of the pump light was 1.58 eV, very near to the absorption peak at ~2 eV, as shown by the red line in Fig. 1(d). As mentioned above, the second peak is assigned as a charge transfer from the O $2p$/Co t_{2g} band to the empty Co e_g band, so the photoexcitation can generate

e_g carriers and probably drives the change of the spin state and resultant I-M transition.

The final issue to be discussed is the dynamics of the metallic state after the photoirradiation. The inset to Fig. 3(a) shows the time profile of $\Delta R/R$ at 0.5 eV. Immediately after photoillumination, $\Delta R/R$ showed a sudden jump due to the photoinduced transition, as mentioned before. After the sharp rise, $\Delta R/R$ showed a small decay, probably because of the suppression of γ, and after $\sim$1 ps it gradually increased. This clearly indicates that the photoinduced metallic region in PCCO showed a further evolution even after $\sim$1 ps.

In Fig. 3(a), we show the time dependence of $\Delta R/R$ from 0 to 50 ps over a wide photon energy region, 0.5–2.0 eV. At 0.5 eV, after the sudden jump, $\Delta R/R$ gradually increased and saturated at $\sim$20 ps. With increasing photon energy of the probe light, however, the overall magnitude of $\Delta R/R$ gradually decreased, and, more importantly, the time profile showed a broad peak. Above $\sim$30 ps, for all the photon energies, $\Delta R/R$ barely changed with the delay time, indicating saturation of the PIPT. The curious time profile with the conspicuous wavelength dependence is different from those of conventional semiconductors [22] and is characteristic of the cobalt system. It suggests a dynamic variation in the photoinduced metallic state on the picosecond time scale.

One may consider that the successive change in $\Delta R/R$ results from the change of the metallic fraction induced by the photoirradiation, as observed in vanadium dioxide. However, the value of the transient reflectivity around the broad peak in Fig. 3(a) is even larger than those in the insulating and the metallic state, and the model of the macroscopic inhomogeneous media composed of the original insulating and the photoinduced metallic states cannot explain the higher reflectivity. To describe this unconventional time dependence of $\Delta R/R$, we assumed the following variation of the dielectric function:

$$\begin{aligned}\varepsilon(z) &= \gamma\varepsilon^M \quad (0 < z < d^{\mathrm{PI}}) \\ &= \gamma \exp(-(z - d^{\mathrm{PI}})/d)\varepsilon^M \\ &\quad + [1 - \gamma \exp(-(z - d^{\mathrm{PI}})/d)]\varepsilon^I] \quad (d^{\mathrm{PI}} < z).\end{aligned} \tag{2}$$

Here, d^{PI} is the thickness of the photonically created metallic state, as schematically shown in the inset of Fig. 3(b). [See also Fig. 4(b) and 4(c).] Again, by numerically calculating the Fresnel coefficient, we calculated $R(\omega)$ at the surface ($z = 0$) as a function of d^{PI}. (The γ value was fixed at 0.7.) In Fig. 3(b), we show the calculated $R(\omega)$ as a function of d^{PI} up to $d^{\mathrm{PI}} = d^{\mathrm{fin}}$ (130 nm) in the photon energy region 0.5–2 eV. We extrapolated a constant value above d^{fin}. As can clearly be seen, the numerical

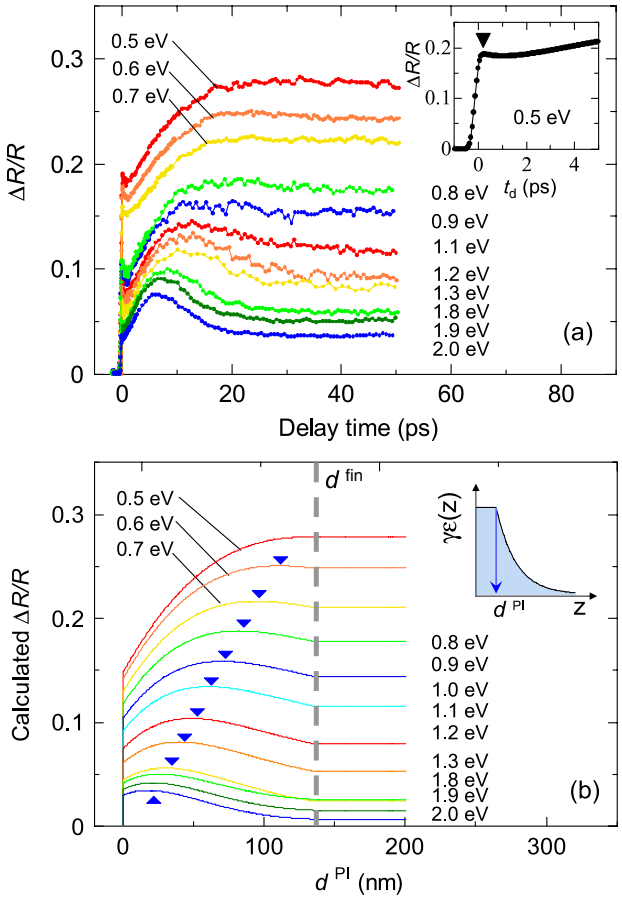

FIG. 3 (color online). (a) Relative change of the reflectivity ($\Delta R/R$) after the photoexcitation from 0.5 to 2.0 eV on the picosecond time scale. The inset shows the initial process of $\Delta R/R$ at 0.5 eV. (t_d denotes a delay time.) (b) Numerically calculated results of d^{PI} dependence of $\Delta R/R$ from 0.5 to 2.0 eV. The inset shows spatial dependence of $\varepsilon(z)$ in Eq. (2). d^{PI} denotes thickness of the uniformed metallic region. See also Figs. 4(b) and 4(c). The upsidedown triangles show the peak of the $\Delta R/R$ profile.

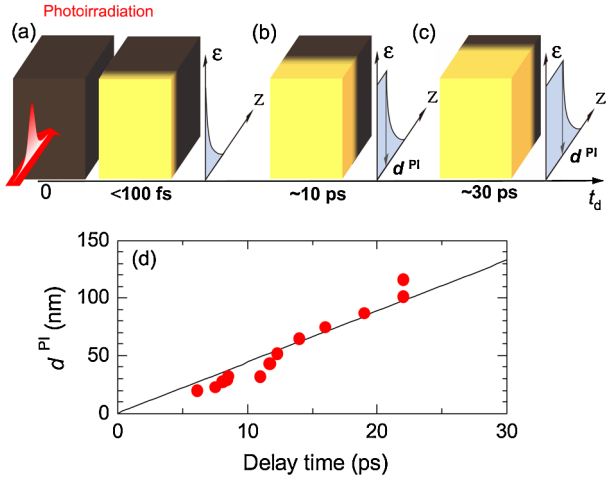

FIG. 4 (color online). (a)–(c) Schematics of the time evolution of the photonically created metallic region, together with the dielectric function (ε) as a function of z [see Eq. (2)]. The yellow or light gray regions show the photoinduced metallic region which propagates itself along z with time evolution. (d) The correlation between the delay time and d^{PI}. The solid line shows the result of the least squares fitting analysis.

calculation [Fig. 3(b)] agrees quite well with the experimentally observed time profiles [Fig. 3(a)], assuming that d^{PI} corresponds to the delay time.

Based on the observed well correspondence between the model calculation and the experimental results, it is quite natural idea that the photonically excited metallic state expands along z according to the increase of delay time. The schematics in Figs. 4(a)–4(c) illustrate the evolution of the photoinduced metallic region as well as the $\varepsilon(z)$. Just after the photoirradiation, the metallic state (yellow or light gray region) has been induced around the surface on the material (dark brown or dark gray region) as shown in Fig. 4(a). As the delay time increases [Fig. 4(b)], the metallic region shows self-propagation along z, indicating the movement of the photoinduced metallic domain whose thickness is characterized by d^{PI}. It seems to be reasonable to assume that the propagation stops around $d^{\mathrm{PI}} \sim 130$ nm [Fig. 4(c)], based on the comparison with the obtained time profile of reflectivity change. The peaks observed in the $\Delta R/R$ profile resulted from the interference of the probe light within the photoinduced metallic region propagating along z.

To estimate the time scale of the development of the photoinduced metallic region, we plotted the relationship between the delay time and the d^{PI} at which $\Delta R/R$ shows a peak in Figs. 3(a) and 3(b) at all photon energies. As shown in Fig. 4(d), d^{PI} linearly increases with the delay time. The velocity was estimated, using least squares fitting analysis, to be $\sim 4.4 \times 10^3$ m/s. This value is comparable to the sound velocity estimated from an elastic constant of a similar cobalt perovskite [23].

It is worth noting here that the propagation speed of $\sim 4.4 \times 10^3$ m/s is faster than that of the expansion of the thermally equilibrium state, because the heat conduction successively occurs after the phonon propagation. In fact, Sokolowski-Tintan *et al.* quantitatively analyzed the velocity of the thermal conduction after irradiation of femtosecond laser pulses [24], indicating that the speed of the heated region is even slower than the above sound velocity by 1 or 2 orders of magnitude. This signals that a simple heating after the photoirradiation cannot explain the fast propagation ($\sim 4.4 \times 10^3$ m/s) of the metallic area. The striking correspondence with the sound velocity implies that the local expansion of the lattice generated by the photoillumination [25] drives the real space propagation of the photoinduced metallic region. Note that even after the damping of the acoustic phonon, the photoinduced metallic region still survives because of the electronic stability of the intermediate metallic state. In this sense, the acoustic phonon in the present system behaves as if it were "negative pressure," which can only be achieved coherently by ultrafast excitation of acoustic phonon wave packets.

In summary, we performed time-resolved reflection spectroscopy on a cobalt perovskite, PCCO, using femtosecond laser pulses. We observed an ultrafast photoinduced insulator to metal transition. The photonically created metallic domain evolves on the picosecond time scale, and model analysis indicates ultrasonic dynamical motion of the photoinduced domain.

The authors thank T. Sato, S. Nozawa, S. Adachi, and M. S. Endo for technical assistance and A. Cavalleri for fruitful discussions. This work was partly supported by Grant-in-Aids for Scientific Research from the MEXT, Japan and G-COE in Tokyo Institute of Technology.

*Present address: The Department of Chemistry, Gunma Univ., Kiryu, Gunma 376-8515, Japan.

[1] *Photoinduced Phase Transitions*, edited by K. Nasu (World Scientific Publishing, Singapore, 2004).
[2] A. Cavalleri *et al.*, Phys. Rev. Lett. **87**, 237401 (2001).
[3] M. Chollet *et al.*, Science **307**, 86 (2005).
[4] P. Baum, D. S. Yang, and H. Zewail, Science **318**, 788 (2007).
[5] K. Miyano *et al.*, Phys. Rev. Lett. **78**, 4257 (1997).
[6] K. Miyasaka *et al.*, Phys. Rev. B **74**, 012401 (2006).
[7] Y. Okimoto *et al.*, J. Phys. Soc. Jpn. **76**, 043702 (2007).
[8] M. Matsubara *et al.*, Phys. Rev. Lett. **99**, 207401 (2007).
[9] M. Rini *et al.*, Nature (London) **449**, 72 (2007).
[10] D. Polli *et al.*, Nature Mater. **6**, 643 (2007).
[11] M. A. Korotin *et al.*, Phys. Rev. B **54**, 5309 (1996).
[12] For example, A. Bousseksou *et al.*, Coord. Chem. Rev. **251**, 1822 (2007), and references cited therein.
[13] S. Tsubouchi *et al.*, Phys. Rev. B **66**, 052418 (2002).
[14] S. Tsubouchi *et al.*, Phys. Rev. B **69**, 144406 (2004).
[15] T. Fujita *et al.*, J. Phys. Soc. Jpn. **73**, 1987 (2004).
[16] T. Saitoh *et al.*, J. Electron Spectrosc. Relat. Phenom. **144**, 893 (2005).
[17] J. Zhou, P. Zheng, and N. L. Wang, J. Phys. Condens. Matter **20**, 055222 (2008).
[18] T. Arima, Y. Tokura, and J. B. Torrance, Phys. Rev. B **48**, 17 006 (1993); M. Imada *et al.*, Rev. Mod. Phys. **70**, 1039 (1998).
[19] D. J. Hilton *et al.*, Phys. Rev. Lett. **99**, 226401 (2007).
[20] In this analysis, we assumed a homogeneous state (or metallic domains are smaller than the wavelength of the probe light) after the photoirradiation.
[21] For example, H. Okamoto *et al.*, Phys. Rev. B **70**, 165202 (2004).
[22] For example, M. Nagai *et al.*, J. Phys. Soc. Jpn. **71**, 2276 (2002); A. J. Sabbah and D. M. Riffe, Phys. Rev. B **66**, 165217 (2002).
[23] S. Murata *et al.*, Physica (Amsterdam) **263B–264B**, 647 (1999).
[24] K. Sokolowski-Tinten *et al.*, Phys. Rev. B **58**, R11 805 (1998).
[25] C. Thomson *et al.*, Phys. Rev. B **34**, 4129 (1986).